Available online at www.sciencedirect.com
SCIENCE DIRECT®
International Journal of Multiphase Flow 31 (2005) 1198–1219
International Journal of Multiphase Flow
www.elsevier.com/locate/ijmulflow

Experimental studies on critical heat flux in vertical tight 37-rod bundles using freon-12

X. Cheng *

Institute for Nuclear and Energy Technologies, Forschungszentrum Karlsruhe, Postfach 3640, D-76021 Karlsruhe, Federal Republic of Germany

Received 29 March 2005; received in revised form 20 June 2005

Abstract

The design of tight-lattice pressurized water reactors requires the knowledge of CHF in tight rod bundles. Experimental investigations on CHF behavior in tight hexagonal 37-rod bundles were performed by using the model fluid Freon-12. About 400 CHF data points have been obtained in a range of parameters: pressure 1.0–2.7 MPa, mass flux 1.4–4.5 Mg/m^2 s and bundle exit steam quality −0.4 to +0.2. It is found that the effect of different parameters on CHF in the tight rod bundle is similar to that in tube geometries. The present test results agree also quantitatively well with the CHF data obtained in tubes of comparable hydraulic diameters. Some in the open literature well known CHF correlations proposed for rod bundles under-predict the test results significantly.

Keywords: CHF; Tight rod bundles; Freon-12

1. Introduction

The critical heat flux (CHF) is the heat flux at which boiling crisis occurs and heat transfer rate deteriorates suddenly. In a system where the heat flux is controlled, e.g. nuclear reactors, an

* Tel.: +49 7247 824897; fax: +49 7247 824837.
E-mail address: xu.cheng@iket.fzk.de

0301-9322/$ - see front matter © 2005 Elsevier Ltd. All rights reserved.
doi:10.1016/j.ijmultiphaseflow.2005.06.003

abrupt rise of the heated wall temperature will take place and, subsequently, cause a failure of the heated surface. Thus, critical heat flux is one of the key design criteria of water cooled nuclear reactors and plays an important role for the safety and economics of nuclear power plants. In spite of a great quantity of experimental and theoretical studies, knowledge of the precise nature of CHF is still incomplete. The great importance of the CHF, coupled with the absence of reliable theoretical modeling, led to a large number of empirical prediction methods. For technical design of nuclear reactors empirical correlations are used which were derived by correlating the available CHF database obtained from particular rod bundles and parameter ranges. An extrapolation of their application to parameters out of this range would result in a large uncertainty.

Since decades, interests have risen in developing tight-lattice pressurized water reactors, to achieve a high conversion ratio, and subsequently, to improve the fuel utilization (Oldekop et al., 1982; Iwamura et al., 1999). Most recently, tight-lattice configuration was also proposed for next generation water cooled reactors at supercritical pressure conditions (Oka and Koshizuka, 2000). A detailed literature survey indicated that experimental as well as theoretical works on CHF for tight hexagonal rod bundles under high pressures and high mass fluxes are scarce. Although experimental studies in small rod bundles were conducted at various institutions (Cheng and Müller, 1998; Okubo, 2000), it has to be pointed out that the effect of cold walls on the distribution of thermal-hydraulic parameters in interior sub-channels is large in such small rod bundles. A direct extrapolation of the test results in small rod bundles to a prototypical rod bundle is not acceptable. Therefore, experimental investigation on CHF in large rod bundles is inevitable for the design of tight-lattice rod bundles.

A program of experimental and analytical investigations on CHF behavior in tight rod lattices was launched at the Institute for Nuclear and Energy Technologies of the Research Center Karlsruhe, in cooperation with the Technical University Braunschweig and Framatome ANP (former KWU/Siemens). Experiments using geometrically identical 37-rod bundles for two different fluids (water, Freon-12) were performed for assessing fluid-to-fluid scaling laws. The experiment in water was conducted by Framatome ANP (Bethke, 1992), whereas the experiment in Freon-12 was performed at the KRISTA test facility of the Research Center Karlsruhe. In this paper the experimental work on the Freon-cooled 37-rod bundle is presented. The effect of different parameters on CHF is analyzed. Some CHF correlations available for rod bundles are assessed with respect to their applicability to tight rod bundles. The test data in bundles were compared with the test data obtained in circular tubes of comparable hydraulic diameters.

2. Experimental approach

The KRISTA test facility, shown schematically in Fig. 1, is used to perform CHF tests in various test sections. Freon-12 was used as working fluid due to its low latent heat, low critical pressure and well known properties. The test loop was constructed for pressure up to 3.5 MPa, mass flow rate up to 14 kg/s and electrical power up to 850 kW. The KRISTA test facility consists of two separate loops which are interconnected via the Freon storage tank and the purification system. A refrigeration system connected to heat exchangers provides a wide range of inlet temperature. The large loop (left part in Fig. 1) is used for the 37-rod bundle tests.

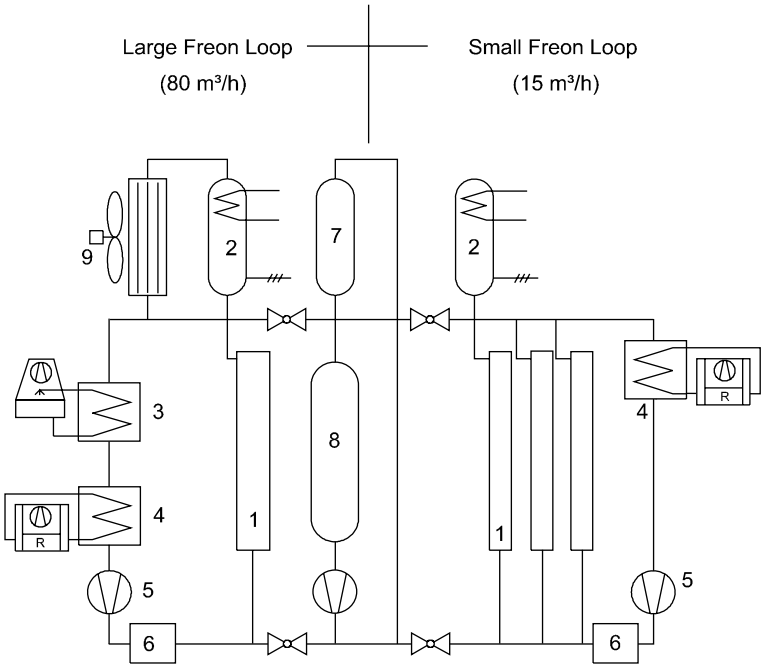

Fig. 1. KRISTA test facility. 1—Test section, 2—Pressurizer, 3—HEX connected to cooling tower, 4—HEX connected to refrigeration system, 5—Pump, 6—Preheater, 7—Purification system, 8—Freon-12 storage tank.

Details of the 37-rod test section are shown in Fig. 2. The total length of the rod bundle is 1240 mm of which 600 mm is heated. The grid spacers are arranged at axial intervals of 300 mm. The closest upstream grid spacer is, therefore, positioned 300 mm upstream from the end of the heated length. This distance is more than 60 times of the bundle hydraulic diameter (4.8 mm), so that the influence of the grid spacer on CHF is negligible small, compared to a bare bundle (Groeneveld et al., 1986). The outer pressure vessel is designed for pressure up to 4.0 MPa. Thermocouples are installed inside the channel wall and permit an accurate determination of the heat balance.

Fig. 3 shows the cross-section of the 37-rod bundle. The test bundle is vertically arranged. Although a large number of CHF experiments in 37 rod bundles were carried out in the past in the framework of the CANDU fuel assembly development (Nickerson, 1982), those bundles were horizontally oriented and their geometric arrangement with round channels was different from the present one. In the present study, the rod diameter and the pitch are 9.0 mm and 10.6 mm, respectively. The rod-to-wall clearance is 1.2 mm. The six corner rods have a diameter of 10.2 mm. The radial power distribution within the bundle was chosen to be identical to that of the water cooled bundle (Bethke, 1992), i.e. the heating power of the seven central rods is 20% higher than that of other 24 rods. The six corner rods are unheated. This radial power distribution ensured that boiling crisis would occur at the inner seven rods. The fuel rod simulators are electrically indirectly heated and have a uniform axial heat flux. To detect the CHF occurrence thermocouples (0.5 mm outer diameter) are embedded in grooves inside the cladding. A plasma spraying process and a subsequent polishing provides a smooth outer surface of the cladding.

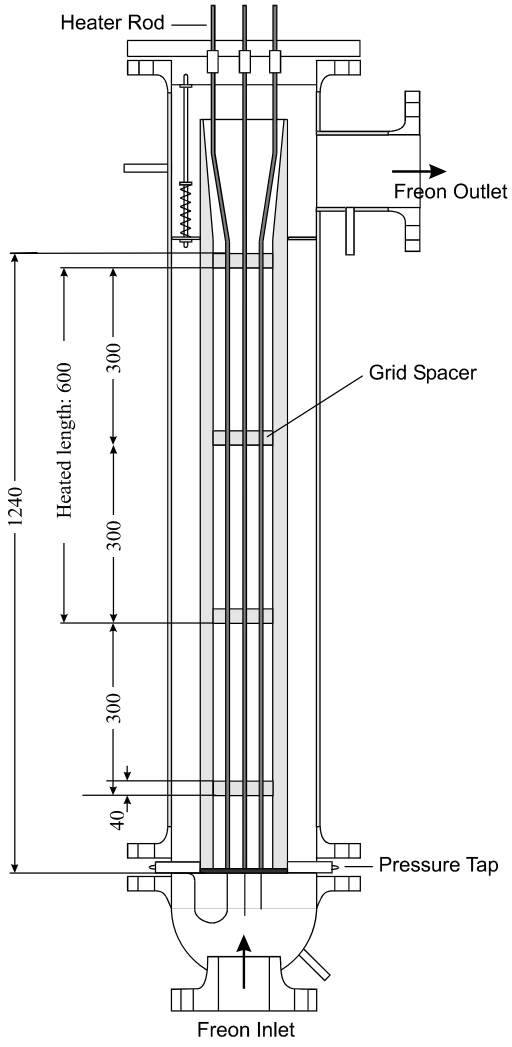

Fig. 2. 37-rod bundle test section.

In each of the seven inner rods eight thermocouples were installed. The junctions were located about 15 mm upstream from the end of the heated length.

Before experiments, Freon-12 from the storage tank is circulated through the purification system until a high purity is obtained. The purified fluid is then filled into the test loop. Both heat exchangers are put into operation and cool down Freon-12 in the test loop. The pressure in the test loop is elevated by turning on the heater which is located in the lower part of the pressurizer and immerged by liquid Freon-12. After the pressure in the test loop reaching a certain level, the hermetic pump is put into operation. The expected value of the fluid temperature at the test channel inlet is obtained by controlling the heating power of the preheater, the thermal-hydraulic parameters of the secondary side of the heat exchangers. The pressurizer maintains the channel outlet pressure constant. The mass flow rate is adjusted by means of control valves.

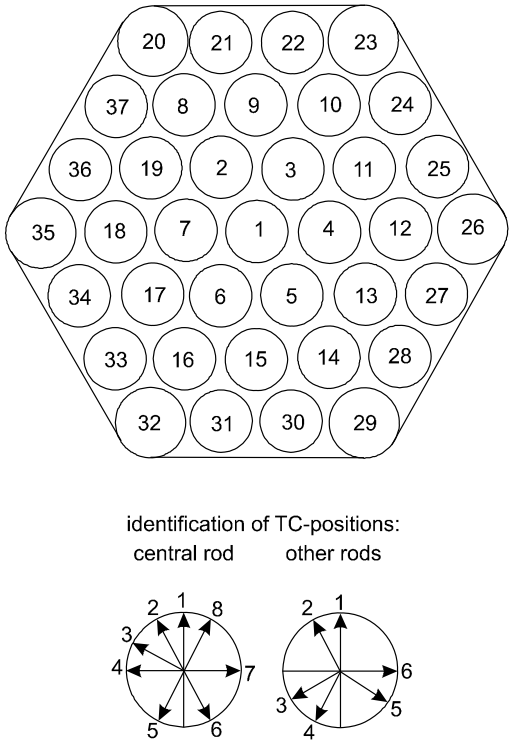

Fig. 3. Cross-section of the 37-rod bundle.

Experiments are performed by holding the test section outlet pressure, inlet temperature and mass flow rate constant, while the heat power is increased at first rapidly to about 80% of the critical heat flux and then slowly and stepwise. The time interval between power steps is long enough, so that any transient effect can be excluded. After each step of power rise flow parameters must be adjusted again to their expected values. The power supply is shut-off automatically, when one of the measured wall temperatures exceeds the given limiting values (e.g. 120 °C), which is well above the saturating temperature and still sufficiently low to avoid chemical decomposition of Freon-12. Boiling crisis is considered to occur when one of the thermocouples shows a temperature value 30 °C higher than the saturation temperature. The test process is controlled by an on-line computer system which registers up to 256 separate channels with a maximum processing frequency of 50 kHz.

For each test run errors of different parameters are analyzed. The error sources considered are mainly:

- measuring instruments,
- fluctuation of measured parameters,
- magnitude of the last power step,
- geometry of the test section,
- heat loss to environment,
- data processing system.

The uncertainty of measuring instruments is determined by the manufacturer's specifications and the calibration results. The fluctuation of the measured parameters and the magnitude of the last power step are evaluated according to the experimental records. The uncertainty of individual events consists of two parts, i.e. systematic error and random error. Normally a variable Z is dependent on several independent variables Z_i:

$$Z = f(Z_1, Z_2, \ldots, Z_n) \tag{1}$$

The systematic error e_s of the variable Z is then function of the systematic errors $e_{s,i}$ of the independent variables Z_i and can be determined by

$$e_s = \frac{\partial f}{\partial Z_1} e_{s,1} + \frac{\partial f}{\partial Z_1} e_{s,2} + \cdots + \frac{\partial f}{\partial Z_1} e_{s,3} \tag{2}$$

Assuming that the random errors of the independent variables obey the Gaussian profile $N(\sigma_i^2, 0)$, the resulted random error of the variable Z has also a Gaussian profile $N(\sigma^2, 0)$ with

$$\sigma^2 = \left(\frac{\partial f}{\partial Z_1}\sigma_1\right)^2 + \left(\frac{\partial f}{\partial Z_1}\sigma_2\right)^2 + \cdots + \left(\frac{\partial f}{\partial Z_1}\sigma_n\right)^2 \tag{3}$$

In the present study, the 2σ-criterion, i.e. 95% probability, was applied. Thus, the error range of the variable Z is given by

$$e = e_s \pm 2\sigma \tag{4}$$

The resulted error range of some important parameters is given as below:

Bundle exit pressure $P_{ex} < 0.02$ MPa
Bundle mass flux G (kg/m^2 s) $< 2.5\%$
Inlet temperature $T_{in} < 1.2$ °C
Local heat flux, q, (kW/m^2) $< 1.0\%$

For sub-channel flow conditions such as local mass flux and local steam quality, the accuracy of a sub-channel code plays the dominant role.

Table 1 summarizes the test matrix. The tests performed cover a wide range of conditions. The pressure is varied from 1.0 MPa to 2.7 MPa which corresponding to an operating pressure range in water from 7.0 MPa to 16.0 MPa, and covers the values used in nuclear reactors. The lower limit of the system pressure is determined by the capacity of the test facility. To obtain a sufficient large subcooling at the test channel inlet, the minimum pressure in the present work is about 1.0 MPa. The bundle mass flux varies in the range from 1.4 to 4.5 Mg/m^2 s. The equivalent mass flux in water is ranging up to about 6 Mg/m^2 s.

The selection of the heated length 600 mm is based on the following considerations: The critical heat flux is often assumed to be only dependent on the local flow conditions, especially in the low steam quality region. For circular tube geometries it has been found that the influence of the heated length on CHF is negligible small, when the ratio of the heated length to the hydraulic diameter exceeds a limit value, e.g. 20 (Cheng et al., 1997). For rod bundle geometries the effect of the heated length on CHF was less investigated. With the heated length 600 mm the ratio of the heated length to the hydraulic diameter of the bundle is about 130. Furthermore, the presence of

Table 1
Test matrix

Parameters	Ranges
Rod diameter (mm)	9.0
Pitch to diameter ratio	1.178
Heated length (mm)	600
Total bundle length (mm)	1240
Intervals of grid spacers (mm)	300
P (MPa)	1.0–2.7
G (Mg/m^2 s)	1.4–4.5
T_{in} (°C)	−10 °C to T_{sat}

grid spacers would reduce the flow upstream effect (upstream of spacers) on the local flow parameter distribution. Therefore, the influence of the heated length on CHF could be negligibly small. Moreover, with this heated length selected, it is expected that for as many test points as possible the exit steam quality will fall into the range from −0.2 to +0.2, which is of interest for nuclear reactor applications.

3. Experimental results and discussions

About 400 test points have been obtained which cover a range of the bundle average exit steam quality from −0.40 to +0.20. The test data obtained at a bundle exit pressure of 2.3 MPa are listed in Table 2. Further test data can be made available by contacting the present author.

In rod bundle geometries CHF results can be presented either by bundle average conditions or by sub-channel flow conditions. In the first approach the directly measured data are taken, whereas in the second approach, a sub-channel analysis code is required to obtain local flow conditions.

3.1. Test results based on bundle average parameters

Fig. 4 shows the test results presented with the bundle average parameters, i.e. the critical bundle power versus the bundle inlet steam quality at various bundle exit pressures and bundle average mass fluxes. Generally, it is seen that the bundle critical power increases with decreasing inlet steam quality and increasing mass fluxes. A larger range of inlet steam quality could be realized at higher pressures due to higher saturating temperatures. The scattering of the test data at high pressures is smaller than that at lower pressures. This is mainly due to a smaller pressure fluctuation at high pressure conditions.

Fig. 5 shows the bundle critical power versus the bundle exit steam quality. At the pressure 1.0 MPa, the effect of mass fluxes is small. By increasing the exit pressure, the effect of mass fluxes becomes evident. For the range of the bundle exit steam quality presented, a lower bundle exit steam quality leads to a higher bundle critical power. The effect of steam quality might change, if one extrapolates the test data to higher steam qualities.

Table 2
Some CHF test data

Test-ID	P_{ex}	G_B	T_{in}	CHF_B
46	2.345	1452.9	6.36	0.21
47	2.359	1443.5	6.13	0.21
48	2.334	1440.3	6.75	0.209
49	2.345	2162.5	8.2	0.283
50	2.363	2160.2	6.75	0.283
51	2.354	2177.3	6.13	0.283
52	2.337	2896.3	9.6	0.349
53	2.359	2905.3	8.43	0.352
54	2.359	2884.8	7.97	0.354
55	2.372	3582.3	7.64	0.421
56	2.35	3626.4	8.99	0.418
57	2.35	3588.2	8.45	0.419
58	2.372	4421.9	8.17	0.488
59	2.363	4360.1	8.78	0.488
60	2.372	4437.4	8.4	0.483
61	2.35	4309	20.8	0.419
62	2.354	4317.2	19.98	0.427
63	2.354	4332.5	20.8	0.424
64	2.346	3592.2	20.18	0.363
65	2.345	3577.3	20.8	0.363
66	2.337	3609	19.39	0.365
67	2.346	2867.2	21.2	0.307
68	2.363	2841.3	19.37	0.306
69	2.341	2846.7	19.6	0.307
70	2.323	2124	19.39	0.245
71	2.345	2182.7	19.52	0.248
72	2.35	2174.9	20.18	0.248
73	2.332	1462.1	20.41	0.187
74	2.345	1474.1	20.8	0.186
75	2.328	1477.1	20.18	0.186
107	2.383	1535.4	−0.99	0.232
108	2.35	1533.7	−0.18	0.231
109	2.363	1529	−0.58	0.231
110	2.35	2220.4	3.08	0.298
111	2.345	2238.7	1.04	0.309
112	2.359	2254.9	0.64	0.308
113	2.354	2974.7	2.67	0.379
114	2.354	2998.8	1.45	0.382
115	2.354	3014.9	0.23	0.391
116	2.359	3777.7	0.84	0.462
117	2.367	3751.7	−0.38	0.462
118	2.367	3704.7	0.23	0.462
119	2.38	4545.1	−0.38	0.536
120	2.367	4551.6	−0.28	0.538
121	2.38	4573.7	−0.18	0.534
212	2.289	1454.5	−0.55	0.214
213	2.298	1457.8	−0.04	0.213

(*continued on next page*)

Table 2 (*continued*)

Test-ID	P_{ex}	G_B	T_{in}	CHF_B
214	2.289	2158.2	−0.24	0.288
215	2.307	2141.2	−1.36	0.291
216	2.294	2862.9	−0.24	0.365
217	2.289	2860.3	−0.04	0.364
218	2.294	3563.8	0.98	0.434
219	2.298	3560.1	0.57	0.437
220	2.298	4228.4	2.4	0.495
221	2.298	4207.6	2.2	0.493
222	2.274	4288.3	10.54	0.46
223	2.27	4254.5	10.75	0.458
224	2.283	3613.2	9.93	0.398
225	2.287	3626.3	10.13	0.399
226	2.261	2833.7	10.54	0.326
227	2.278	2807.9	10.74	0.322
228	2.27	2161.2	10.95	0.26
229	2.287	2128.4	10.95	0.26
230	2.296	1424.2	10.54	0.19
231	2.278	1415	10.74	0.188
232	2.292	1430.1	20.1	0.174
233	2.3	1422.4	19.9	0.173
234	2.274	2105.7	20.92	0.231
235	2.278	2097.4	20.92	0.229
236	2.278	2838.3	21.12	0.292
237	2.274	2823.6	20.51	0.292
238	2.274	3569.5	21.12	0.358
239	2.274	3549.9	20.31	0.358
240	2.278	4199.7	20.92	0.411
241	2.27	4185.6	20.82	0.413
242	2.263	4169.1	30.58	0.36
244	2.274	3535.5	29.77	0.317
245	2.274	3530	29.87	0.314
246	2.292	2824.4	29.57	0.263
247	2.287	2825.5	29.87	0.263
248	2.278	2126.1	30.07	0.212
249	2.283	2129.4	29.67	0.211
250	2.292	1403.9	30.48	0.157
251	2.292	1426.9	30.48	0.159
252	2.278	1412.9	40.25	0.139
253	2.3	1402.7	39.94	0.139
254	2.274	2145.7	39.94	0.184
255	2.274	2144.2	40.25	0.185
256	2.278	2836	39.94	0.225
257	2.274	2827	40.25	0.224
258	2.268	3462.7	40.45	0.269
259	2.278	3470.1	39.84	0.273
260	2.278	4231.9	40.25	0.314
261	2.257	4228.5	40.86	0.314
262	2.278	4180.5	50.22	0.263
263	2.274	4208	50.22	0.267

Table 2 (*continued*)

Test-ID	P_{ex}	G_B	T_{in}	CHF_B
264	2.268	3506.7	49.61	0.232
165	2.278	3541	49.81	0.231
266	2.265	2817.5	49.91	0.193
267	2.274	2827.6	50.62	0.193
268	2.278	2075.2	50.22	0.155
269	2.283	2095.7	50.22	0.156
270	2.278	1429.1	50.22	0.123
271	2.292	1438.4	50.83	0.123
272	2.309	1408.9	59.98	0.108
273	2.322	1420.3	59.98	0.109
274	2.296	2113.6	59.48	0.134
275	2.294	2109	59.78	0.135
276	2.285	2887.2	59.98	0.163
277	2.285	2918.4	60.09	0.164
278	2.289	3514.1	59.98	0.186
279	2.274	3513.1	60.09	0.185
280	2.285	4153.7	60.59	0.21
281	2.289	4183.2	59.88	0.214
282	2.318	4181.2	70.56	0.163
283	2.314	4247.3	69.85	0.167
284	2.32	3501	69.65	0.151
285	2.32	3559.8	69.65	0.15
286	2.314	2854.4	69.85	0.133
287	2.331	2829.8	69.65	0.134
288	2.322	2143.5	69.75	0.115
289	2.335	2148.9	70.05	0.112
290	2.357	1420	69.95	0.093
291	2.34	1429.3	69.95	0.093

Test-ID: Test identification number; P_{ex}: Pressure at bundle exit, MPa; G_B: Bundle mass flux, kg/m^2 s; T_{in}: Temperature at bundle inlet, °C; CHF_B: Bundle average heat flux at onset of boiling crisis, MW/m^2.

Fig. 6 indicates the effect of pressure on critical power. At low mass fluxes, the effect of pressure on critical power is significant. A lower pressure leads to a higher critical power. The effect of pressure reduces with increasing mass fluxes. At high mass fluxes, e.g. 4.2 Mg/m^2, the effect of pressure is negligibly small at steam qualities $x_{ex} > -0.2$. The pressure influence on CHF is a consequence of the fluid properties: a higher pressure leads to (1) a lower value of latent heat and a higher rate of evaporation which in turn leads to a lower CHF, (2) a higher vapor density which tends to reduce the void fraction and increase the value of CHF, (3) a lower surface tension which in consequence leads to a lower value of CHF. Thus the influence of pressure on CHF depends on which of the factors prevail. The test results show that at low steam qualities an increasing pressure leads to a lower CHF. In this region the effects of lower latent heat and lower surface tension prevail over the effect of higher vapor density. These results agree well with the results proposed in pool boiling. At high steam qualities an increase in the CHF is observed by increasing pressure. In this case, the effect of increasing steam density is dominating over other effects.

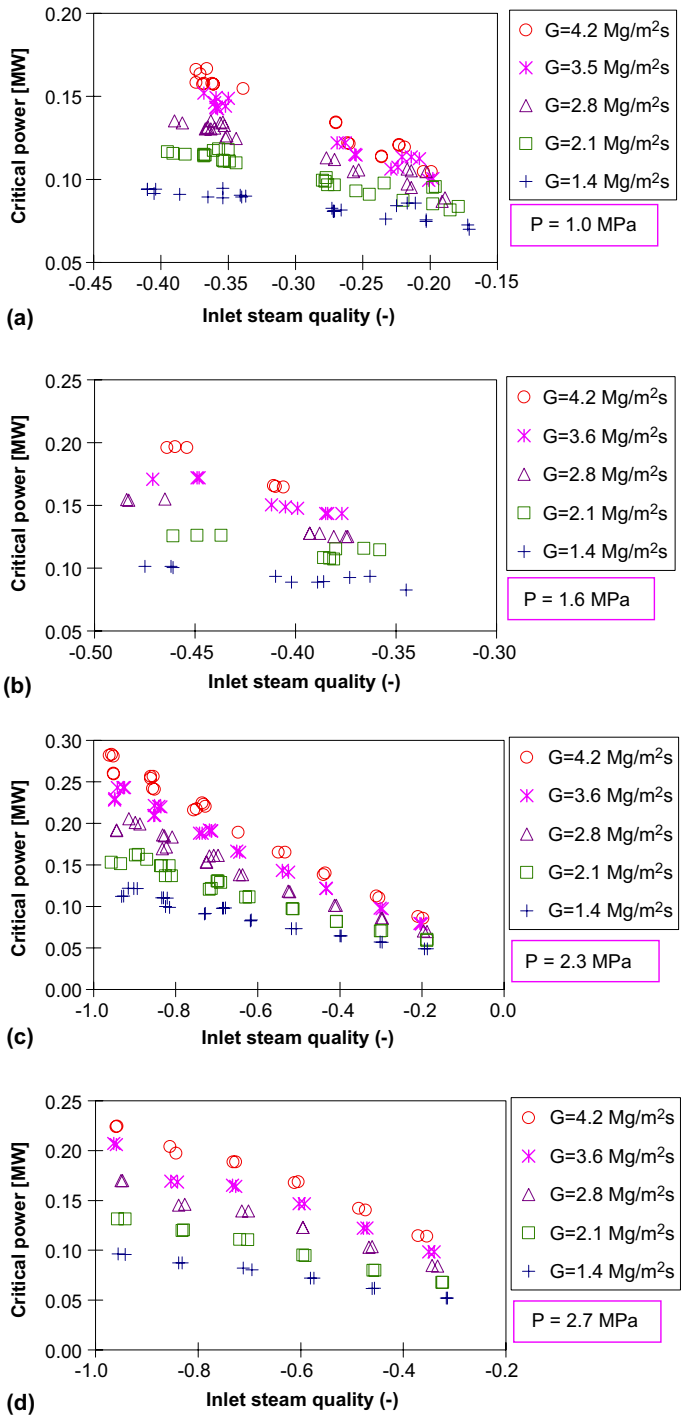

Fig. 4. Critical power versus inlet steam quality at various mass fluxes. (a) $P = 1.0$ MPa, (b) $P = 1.6$ MPa, (c) $P = 2.3$ MPa and (d) $P = 2.7$ MPa.

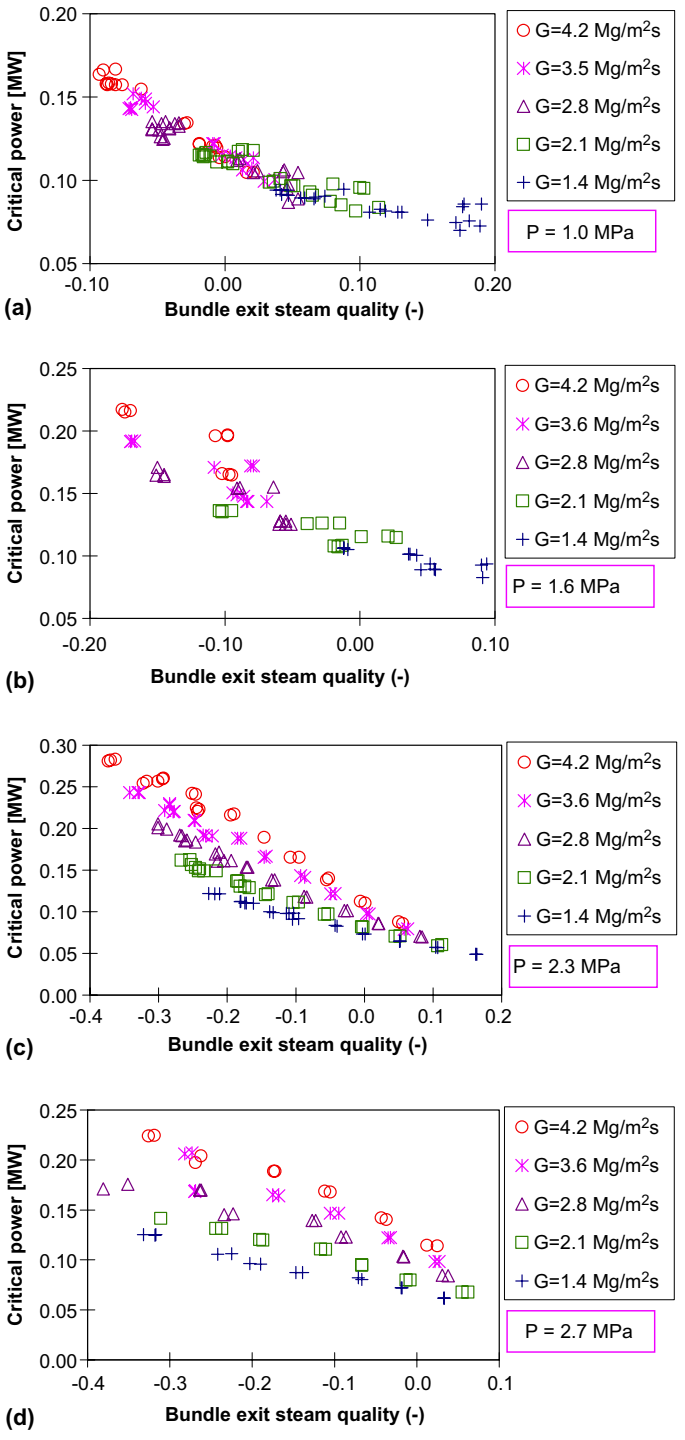

Fig. 5. Critical power versus bundle exit steam quality at various mass fluxes. (a) $P = 1.0$ MPa, (b) $P = 1.6$ MPa, (c) $P = 2.3$ MPa and (d) $P = 2.7$ MPa.

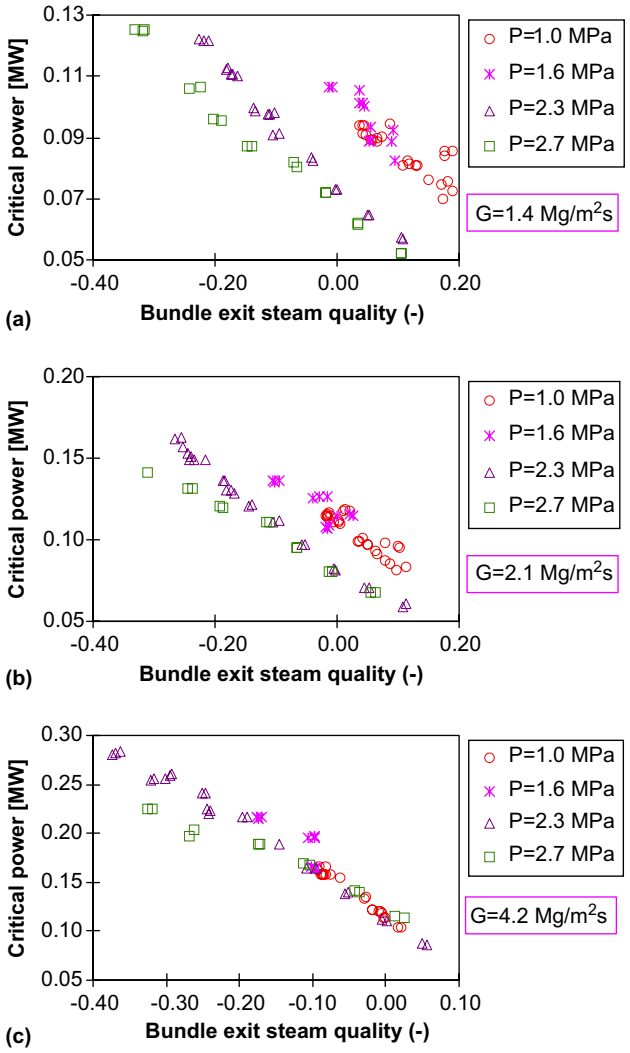

Fig. 6. Critical power versus bundle exit steam quality at various pressures. (a) $G = 1.4$ Mg/m^2 s, (b) $G = 2.1$ Mg/m^2 s and (c) $G = 4.2$ Mg/m^2 s.

The experimental findings described above, i.e. the effect of steam quality, mass flux and pressure on critical power, agree qualitatively well with the experimental observation made in circular tubes (Cheng et al., 1997).

3.2. Test results based on sub-channel parameters

It is often assumed that boiling crisis is a local phenomenon. Critical heat flux depends on local conditions. For a better understanding of the physical mechanisms of boiling crisis the use of sub-

channel conditions is a more favorable method, especially in rod bundles where strong thermal imbalance appears. To achieve sub-channel flow conditions the sub-channel analysis code COBRA-IV-TUBS is used. More details about this code and some physical models used were documented by Bethke (1992). The previous studies of the present author (Cheng and Müller, 1998) indicates that the accuracy of sub-channel analysis codes depends strongly on the reliability of physical models describing the inter-channel exchange of mass, energy and momentum, known as mixing. Inter-channel exchange can be split into two phenomena. First, there is a net mass flux between sub-channels which is caused by radial pressure gradient. Secondly, there is natural mixing causing exchange of enthalpy between neighboring sub-channels but does not result in a net mass flow or a net volume flow. The latter one can be represented by the mixing coefficient β which is defined as the total transversal mass flow caused by natural mixing divided by the mean axial mass flux. The total transversal mass flux consists of a turbulent share and a molecular contribution which, however, can be neglected compared to the turbulent share for high Reynolds numbers. It is well known that the mixing coefficient is dependent on flow conditions and on sub-channel geometry (Rogers and Rosehart, 1972). Nevertheless, experimentally verified models of mixing coefficient in two-phase flow regime are not available up to now.

A sensitivity study was performed to determine the sensitivity of calculated sub-channel flow conditions to the mixing coefficient. Fig. 7 shows the effect of the turbulent mixing coefficient on the local exit steam quality of the hot sub-channel in the 37 rod bundle. A strong effect of the turbulent mixing coefficient on the calculated sub-channel condition is observed. In spite of intensive studies carried out worldwide there exist still deficiencies in analysis of sub-channel flow parameters under high pressure two-phase flow conditions (Wolf et al., 1987). It has to be kept in mind that the accuracy of a CHF prediction method in the rod bundle geometry is coupled with the accuracy of determining sub-channel flow conditions. Based on the test data of turbulent mixing in a tight hexagonal 7-rod bundle (Cheng and Müller, 1998), two mixing coefficient values, i.e. 0.004 of 0.02, have been considered in the present investigation.

Fig. 8 shows the mass flux and the enthalpy gain ratio of the hot sub-channel at the exit elevation. These ratios are defined as:

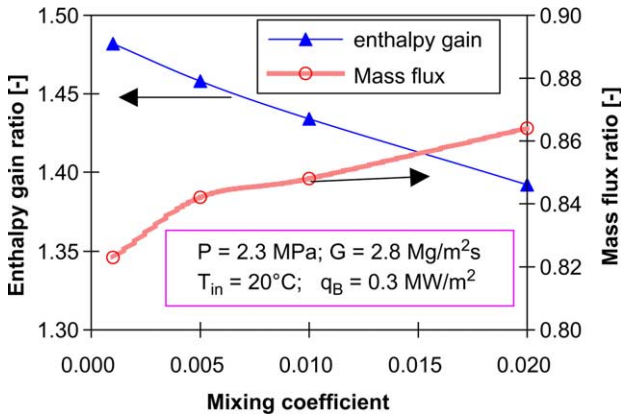

Fig. 7. Effect of mixing coefficient on local parameters of hot sub-channels.

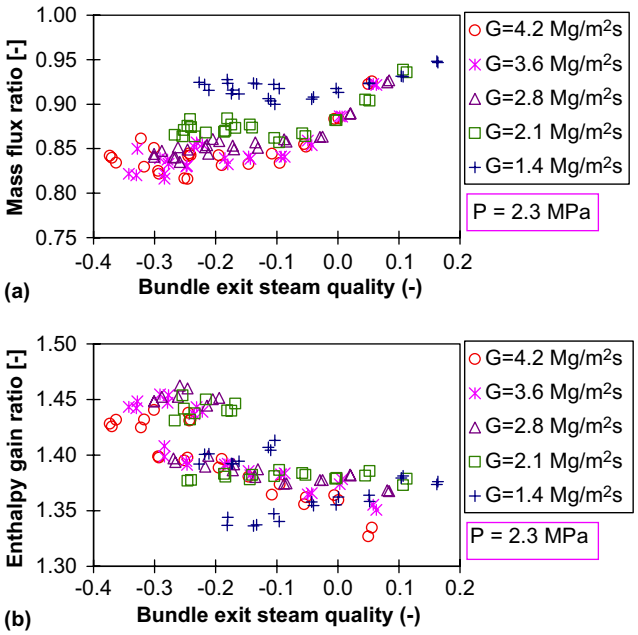

Fig. 8. Mass flux and enthalpy gain in hot sub-channels ($\beta = 0.004$): (a) mass flux ratio and (b) enthalpy gain ratio.

$$\text{mass flux ratio} = \frac{G_1}{G_B} \tag{5}$$

$$\text{enthalpy gain ratio} = \frac{h_{ex,1} - h_{in}}{h_{ex,B} - h_{in}} \tag{6}$$

where G is mass flux, h enthalpy. The subscript 'in' stands for inlet, 'ex' for outlet, '1' for hot sub-channel and 'B' for bundle average values. The exit pressure is 2.3 MPa, and the mixing coefficient is 0.004. For the test points presented in these figures the mass flux in the hot sub-channel is up to 20% lower than the bundle average value, whereas the enthalpy gain in the hot sub-channel is up to 50% higher than the bundle average value.

Fig. 9 presents the local critical heat flux versus the local steam quality which was obtained by using a mixing coefficient of 0.004. Again a large scattering is obtained at low pressures. It has to be pointed out that a data group indicated with one symbol does not represent test data of one identical value of mass flux, but a range of mass fluxes. Generally it shows that the effect of mass fluxes on CHF is small, except at high pressures, e.g. 2.7 MPa.

3.3. Comparison with CHF data in circular tubes

The present author carried out experimental studies of CHF in circular tubes using Freon-12 (Cheng et al., 1997). Fig. 10 gives the comparison of the test data in the 37 rod bundle with those obtained in the 4.2-mm tubes. The hydraulic diameter of the 37-rod bundle is 4.8 mm, comparable

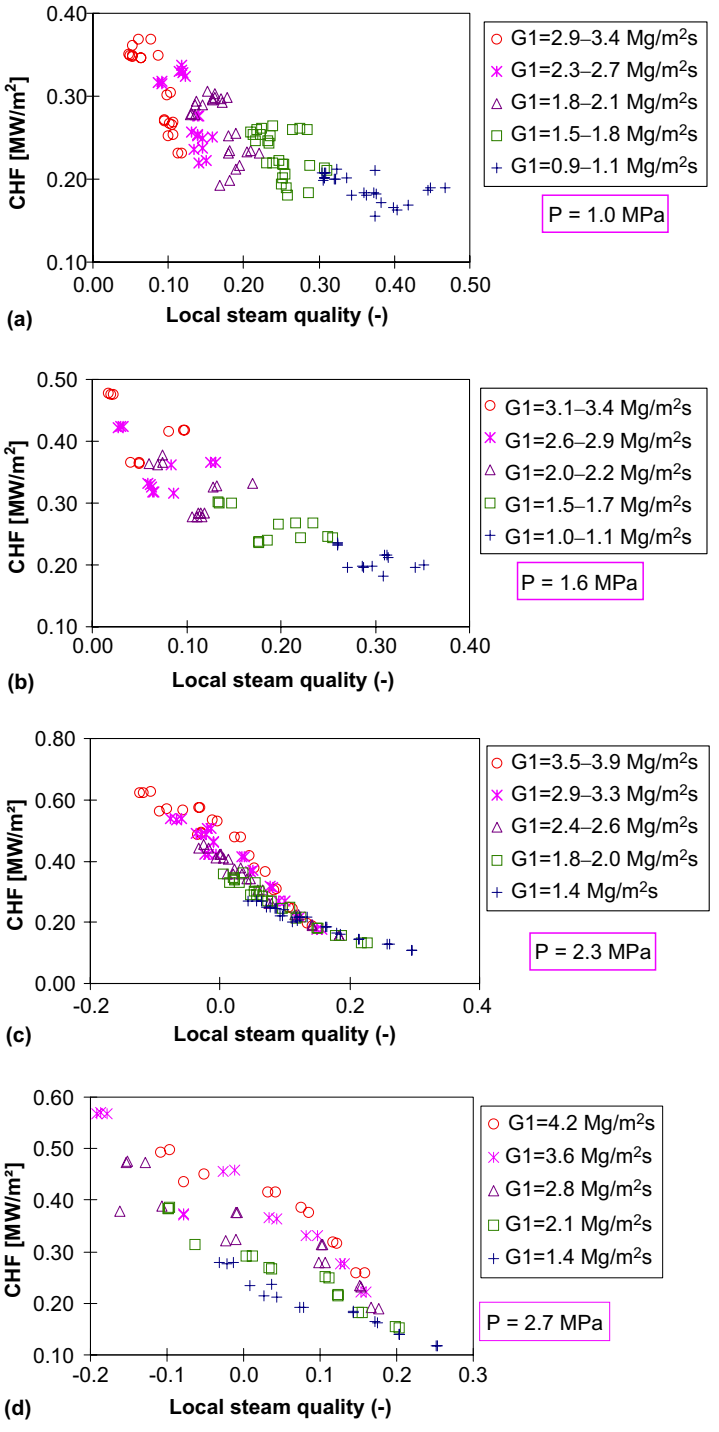

Fig. 9. CHF based on local parameters ($\beta = 0.004$). (a) $P = 1.0$ MPa, (b) $P = 1.6$ MPa, (c) $P = 2.3$ MPa and (d) $P = 2.7$ MPa.

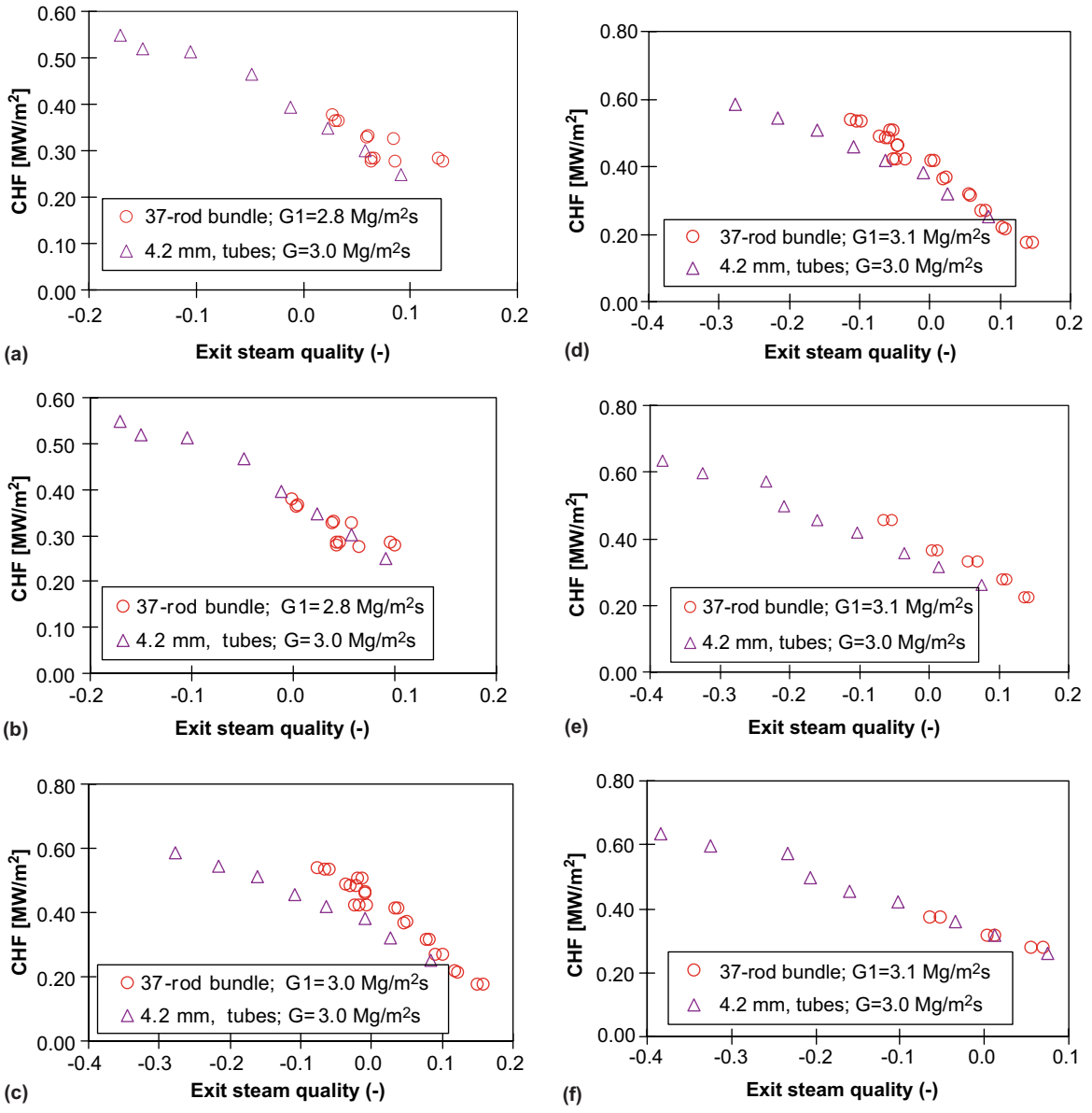

Fig. 10. Comparison of test data in rod bundle with those in 4.2 mm circular tubes. (a) $P = 1.8$ MPa, $\beta = 0.004$; (b) $P = 1.8$ MPa, $\beta = 0.02$; (c) $P = 2.3$ MPa, $\beta = 0.004$; (d) $P = 2.3$ MPa, $\beta = 0.02$; (e) $P = 2.7$ MPa, $\beta = 0.004$ and (f) $P = 2.7$ MPa, $\beta = 0.02$.

to that of the circular tube. The test data shown in Fig. 10 are based on local parameters. In Fig. 10, test data at three pressures using two different values of mixing coefficient are presented. The local mass flux is about 3.0 Mg/m^2 s. It has to be pointed out that similar results are achieved at other values of mass fluxes.

Generally, a good agreement was obtained between the CHF data in the 37-rod bundle and those in circular tubes of comparable hydraulic diameters. At low pressures and small values of mixing coefficient, the CHF test data in bundles are slightly higher than those in circular tubes, whereas at high pressures and large values of mixing coefficient, the CHF data in bundles are slightly lower than those in tubes. An excellent agreement is achieved at low pressures and a large mixing coefficient or at high pressures with a small mixing coefficient.

3.4. Comparison with CHF correlations

Nowadays, there exist a large number of empirical correlations that have been developed by correlating available CHF databases obtained from particular flow channel geometries and parameter

Table 3
CHF prediction methods and their valid parameter ranges

	Fluid	P, MPa	G, Mg/m^2 s	X_{ex}
EPRI-1	Water	0.4–17.0	0.3–5.5	−0.25–0.75
KfK-3	Water	2.7–14.0	⩽5.4	−0.44–0.96
GSM.6[a]	Water/R12	1.2–2.9	2.0–9.0	−0.20–0.40

[a] The parameter range given is valid for Freon-12 conditions.

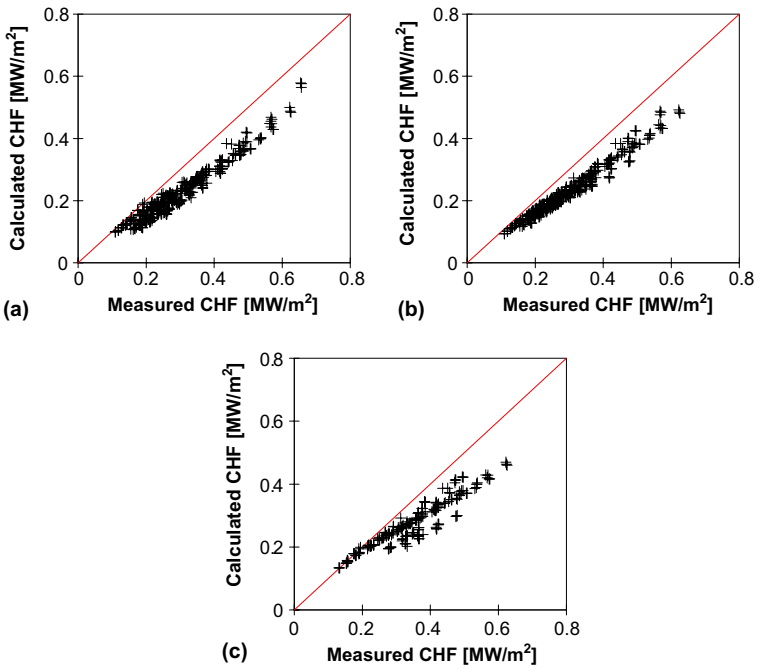

Fig. 11. Comparison of test results with CHF correlations (HBM method, $\beta = 0.02$). (a) KfK-3 correlation, (b) EPRI-1 correlation and (c) GSM.6 correlation.

ranges (Cheng and Müller, 2003). However, experimental investigations on CHF were performed for each specific design of fuel elements and operating conditions, to derive prediction methods for specific design conditions. Obviously, many correlations of rod bundle CHF are in existence. However, most of them are of proprietary nature and not available in the open literature.

Table 3 summarizes four CHF prediction methods selected in the present work to show to what extent they can reproduce the test results. The EPRI-1 correlation (Fighetti and Reddy, 1983) has been developed for square LWR element lattice by using more than 5000 test points in 20 different rod bundles. The KfK-3 correlation of Dalle Donne (1991) has been derived on the basis of the WSC-2 correlation (Bowring, 1979) and by adapting some test data obtained in hexagonal tight lattices. The GSM.6 correlation of Courtaud et al. (1988) has been developed by using the test data obtained in tight hexagonal 19-rod bundles by using both Freon-12 and water.

Except for the GSM.6 correlation, other two correlations indicated in Table 3 are derived for water conditions. To compare these prediction methods with the experimental data in Freon-12 fluid-to-fluid scaling laws are needed, to transfer the test data obtained in the model fluid Freon-12 to the prototypical fluid (water). A thorough assessment of the existing scaling laws was also made by Katsaounis (1981) and Cheng et al. (1997). It was concluded that the fluid-to-fluid scaling law of Ahmad (1973) is well suited for fluid-to-fluid modeling in circular tubes and for square type wide rod bundles. In the present paper, the scaling law of Ahmad was used to transfer the test data in Freon-12 to water equivalent conditions.

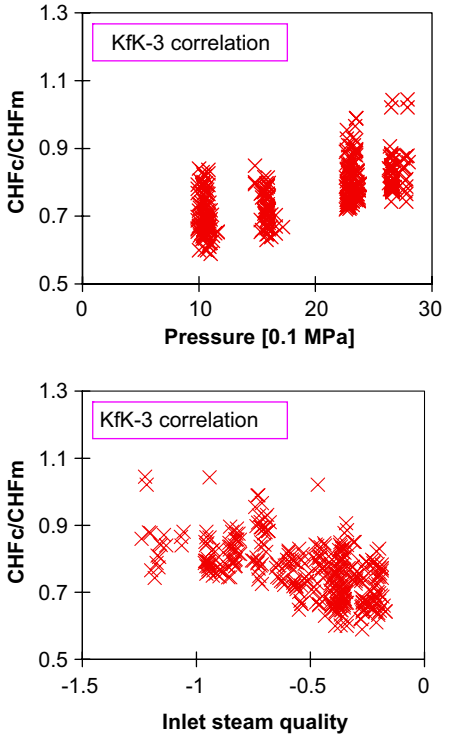

Fig. 12. Comparison of the test results with KfK-3 correlation (HBM method, $\beta = 0.02$) CHF_c: calculated CHF CHF_m: measured CHF.

Fig. 11 compares the test results with the three CHF correlations. The comparison is based on the heat balance method HBM (Siman-Tov, 1996). The local sub-channel parameters are determined using a mixing coefficient of 0.02. It can be seen that all three correlations under-predict the test results significantly. On the average, the calculated CHF values are about 25% lower than the measured results. A detailed assessment of different fluid-to-fluid scaling laws available in the literature shows that no significant improvement can be achieved by using other scaling laws than the scaling law of Ahmad. The deviation becomes larger, if a smaller value of mixing coefficient (0.004) is applied to calculate the sub-channel parameters.

Fig. 12 shows the ratio of the measured CHF to the calculated CHF, using the KfK-3 correlation, in dependence on pressure (Fig. 12a) and inlet steam quality (Fig. 12b). Obviously, a much stronger under-prediction is observed at low pressures. An improved agreement is obtained at low inlet steam qualities or high inlet subcooling. Similar conclusion can also be achieved for the EPRI-1 correlation.

The above comparison indicates a deficiency in accurate CHF correlations proposed for tight rod bundles. However, it is not worth making efforts to develop new correlations for the present Freon-12 test condition, due to insufficient test data and limited importance in application. Based on the comparison with the CHF data in tubes, CHF prediction methods proposed for tubes, e.g. CHF look-up tables, would be recommended to tight hexagonal rod bundles using local thermal-hydraulic conditions.

4. Conclusions

The great importance of the critical heat flux, coupled with the scarcity of knowledge of the mechanisms concerned, led to the requirement of experimental investigations for each specific design of fuel bundles. In the present paper, experimental studies on CHF in tight hexagonal 37-rod bundles were carried out. The model fluid Freon-12 was used as working fluid due to its low latent heat, low critical pressure, well known properties and intensively investigated fluid-to-fluid modeling for water and Freon-12. About 400 data points were obtained over a large range of parameters: pressure 1.0–2.7 MPa, mass flux 1.4–4.5 Mg/m^2 s and bundle exit steam quality -0.40 to $+0.20$. The main objectives of the present work are to look insight into the CHF behavior in tight hexagonal bundles; to supplement the CHF database available for rod bundles, especially for tight rod bundles; to assess CHF correlations in the open literature and to provide basic information on CHF for the design of water cooled tight fuel bundles of various reactor concepts, e.g. high conversion PWR (Oldekop et al., 1982), reduced-moderation water reactor (Iwamura et al., 1999) or supercritical water reactor (Oka and Koshizuka, 2000). Based on the results presented in this paper, the following specific conclusions can be drawn:

- A CHF database covering a large parameter range was obtained for investigating CHF behavior and for assessing CHF prediction methods in tight hexagonal rod bundles. Combined with the test data obtained in a geometrically identical rod bundle using water as coolant, the present database can be applied for evaluating and for the development of fluid-to-fluid scaling laws in tight hexagonal rod bundles.

- The effect of different parameters, i.e. pressure, mass flux and steam quality, on CHF is similar to that observed in circular tubes. Quantitatively, a good agreement is achieved between the CHF data in rod bundles and those in circular tubes of comparable hydraulic diameters.
- Some in the open literature well known CHF correlations under-predict the test results significantly, especially at conditions of low pressures and low inlet steam qualities. Applying of different fluid-to-fluid scaling laws does not lead to a significantly improved agreement. However, CHF prediction methods proposed for circular tubes are recommended to the present tight rod bundles using local thermal-hydraulic conditions.

Finally, it has to be pointed out that both analysis of CHF test results and assessment of CHF prediction methods depend strongly on the approach applied. In case using local sub-channel parameters, the reliability of the sub-channel analysis code plays an important role. However, the accuracy of the available sub-channel analysis codes for two-phase flows under high pressures is still limited. One of the main reasons is due to the limited measurement technique to reliably determine the local flow parameters in sub-channels at high pressure conditions. In addition to the development of advanced experimental techniques, numerical analysis using computational fluid dynamics (CFD) codes would make significant contribution to derive more accurate models used in the sub-channel analysis codes. The CFD application to rod bundles is achieving more and more attention worldwide and is also ongoing at the Forschungszentrum Karlsruhe (Cheng and Laurien, 2005).

References

Ahmad, S.Y., 1973. Fluid-to-fluid modeling of critical heat flux: a compensated distortion model. Int. J. Heat Mass Transfer 16, 641–662.

Bethke, S., 1992. Analysis of critical heat flux in rod bundles (in German). Ph.D. Thesis, Technical University Braunschweig.

Bowring, R.W., 1979. WSC-2: a subchannel dryout correlation for water-cooled clusters over the pressure range 3.4–15.9 MPa. Winfrith: Atomic Energy Establishment, AEEW-R-983.

Cheng, X., Müller, U., 1998. Turbulent mixing and critical heat flux in tight 7-rod bundles. Int. J. Multiphase Flow 24, 1245–1263.

Cheng, X., Müller, U., 2003. Review on critical heat flux in water cooled reactors. Wissenschaftliche Berichte FZKA-6825, Forschungszentrum Karlsruhe.

Cheng, X., Laurien, E., 2005. CFD analysis of heat transfer in supercritical water in different flow channels. GLOBAL-2005, Paper 369, October 9–13, 2005, Tsukuba, Japan.

Cheng, X., Erbacher, F.J., Müller, U., 1997. Critical heat flux in uniformly heated vertical tubes. Int. J. Heat Mass Transfer 40, 2929–2939.

Courtaud, M., Deruaz, R., D'Aillon, L.G., 1988. The French thermal-hydraulic program addressing the requirements of the future pressurized water reactors. Nucl. Technol. 80, 73–82.

Dalle Donne, M., 1991. CHF-KfK-3: a critical heat flux correlation for triangular arrays of rods with tight lattices. Research Center Karlsruhe, KfK-4826.

Fighetti, C.F., Reddy, D.G., 1983. A generalized subchannel CHF correlation for PWR and BWR fuel assemblies. Electric Power Research Institute, EPRI-NP-2609-Vol. 2.

Groeneveld, D.C., Cheng, S.C., Doan, T., 1986. AECL-UO critical heat flux look-up table. Heat Transfer Eng. 7, 46–61.

Iwamura, T., et al., 1999. Research on reduced-moderation water reactor (RMWR), JAERI-Research 99-058.

Katsaounis, A., 1981. Literaturbewertung zur Fluidähnlichkeit für die kritische Heizflächenbelastung. Technical Report GKSS 81/E/10, GKSS-Forschungszentrum Geesthacht GmbH, Germany.

Nickerson, J.R., 1982. Critical heat flux and post-critical heat flux performance of a 6-m, 37-element fully segmented bundle cooled by Freon-12. Report AECL-7695, Chalk River Nuclear Laboratories, Chalk River, Ontario, May 1982.

Oka, Y., Koshizuka, S., 2000. Design concept of once-through cycle supercritical pressure light water cooled reactors. In: Proceedings of SCR-2000, November 6–8, Tokyo, pp. 1–22.

Okubo, T., 2000. Critical heat flux for tight lattice rod bundle, private communication.

Oldekop, W., Berger, H.D., Zeggel, W., 1982. General features of advanced pressurized water reactors with improved fuel utilization. Nucl. Technol. 59, 212–227.

Rogers, J.T., Rosehart, R.G., 1972. Mixing by turbulent interchange in fuel bundles: correlations and inferences. ASME paper 72-HT-53, New York, 1972.

Siman-Tov, M., 1996. Application of energy balance and direct substitution methods for thermal margins and data evaluation. Nucl. Eng. Des. 163, 249–258.

Wolf, L. et al., 1987. Comprehensive assessment of the ISPRA BWR and PWR subchannel experiments and code analysis with different two-phase models and solution schemes. Nucl. Eng. and Des. 99, 329–350.